[1.]Beáta ŠIMEKOVÁ, [2.]Ingrid KOVAŘÍKOVÁ, [3.]Erika HODÚLOVÁ, [4.]Michal ŠIMEK

INFLUENCE OF ELECTRON BEAM OSCILLATION AND HEAT INPUT ON THE QUALITY OF SAF 2205 DUPLEX STAINLESS STEEL WELDS

[1-3.]Department of Welding a Joining of Materials, Faculty of Materials Science and Technology, SLOVAKIA
[4.] First Welding Company, Inc., SLOVAKIA

Abstract: This paper investigates the weldability, metallurgical and mechanical properties of 5 mm thickness plate of SAF 2205 duplex stainless steel joints by electron beam welding (EBW) process. The excellent properties of duplex stainless steels (DSS) are due to their strict composition control and microstructural balance. The ferrite/austenite ratio is often upset in duplex stainless steel weld metals owing to the rapid cooling rates correlated with welding. To achieve the required ferrite/austenite balance and good properties, the welding process and the heat input must be controlled. Each joint obtained by electron beam welding and their individual sub-regions through thickness were characterised by optical microscopy. Distribution of elements in various areas was evaluated by scanning electron microscope (SEM/EDX). On the particular samples was observed microhardness and ferrite/austenite balance. Ultrasonic non-destructive testing was used for quality assessment of EBW duplex steel joints. Electron beam welding has produced weld joints with a significant decrease in austenite zone size. The ferrite/austenite balance of both weld metal and heat affected zone are influenced by heat input which is a function of welding process. This work describes the possibilities how to achieve the weld joints of high quality by using the optimal welding parameters [1,2].
Keywords: duplex stainless steels, electron beam welding, cooling rate, heat input, ferrite/austenite balance

1. INTRODUCTION

This alloy group has been developed over the past 30 years. The development progress has resulted in a range of compositions including lean 22% chromium (Cr) and 25% chromium, which are standard of DSS. These alloys have high strength, good toughness, good corrosion resistance, good weldability, and formability, all of which ease manufacturing mentioned in H.D. Solomon and Bonnefois [3,4]. These alloys combine the strength characteristics of ferritic stainless steels and the corrosion resistance of austenitic stainless steels. They have higher resistance to environmental corrosion than austenitic stainless steels. Dual phase alloying requires lower Ni and Mo contents than single-phase austenitic alloys. The alloys with higher F_{PREN} values are possible through the addition of nitrogen to the alloy. Duplex stainless steels contain up to 22% chromium their key property of value to industry is the material's pitting resistance F_{PREN}, which is typically in the range of 35 to 40. The chromium content of super duplex steel is up to 25% and its pitting resistance F_{PREN} is typically in the range of 40 to 45 say Lippold and all [5-7].

For the improved properties is responsible optimal controlled phase balance which is achieved in the production route through tight composition control and heat treatment However, welding process of DSS has results in a disturbed phase balance. This problem is more significant in power beam welding processes for their low heat input and very fast cooling rates [8]. However the non-destructive inspection of duplex and superduplex steels is a big challenge as those steels, being composed of ferrite and austenite, have some particularities. When using ultrasound, for instance, its waves propagate well in ferrite, but suffer strong attenuation, scattering and refraction in austenite.

The typical microstructure of duplex stainless steel is illustrated in figure 1.

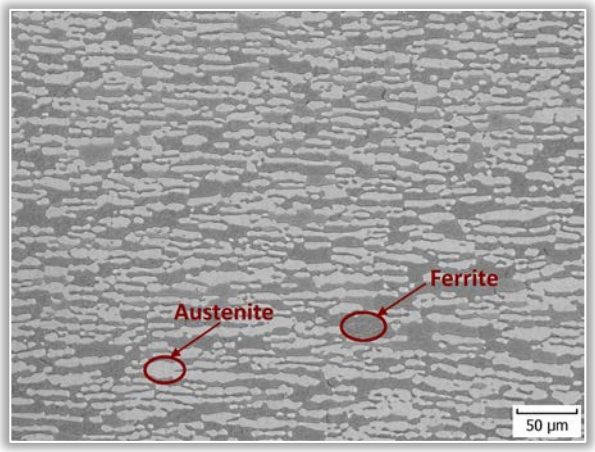

Figure 1. Representative microstructure of the investigated material

2. EXPERIMENTAL

— Composition of duplex stainless steel

The investigated material is a type UNS S32205 (EN 1.4462) steel in the form of 5 mm thickness plate, what composition is given in table 1. The grains grow in microstructure at temperatures above 1050 °C and the ferrite begins to secrete. Opposite changes on the interfaces of ferrite grains are occurred at cooling, but also austenite is formatted intra-granular again. Elongated islands of δ-ferrite and γ-austenite were visible.

Table 1. Chemical composition of duplex stainless steel EN 1.4462

C*	Si*	Mn*	Ni	P*	S*	Cr	Mo	N
0,03	1,00	2,00	4,50-6,50	0,035	0,015	21,00-23,00	2,30-3,50	0,10-0,22

* Maximum content

— Electron beam welding experiments

Welding experiments were done using universal electron beam welder PZ – EZ – ZH3 (illustrated in figure 2) with accelerating voltage 60 kV and power 9 kW. This equipment was constructed by First Welding Company, Inc. For this experiment were made the nine electron beam welds. On the nine keyhole welds was used welding current in the range of 23 - 65 mA with welding speeds from 5 to 30 mm.s^{-1} and average oscillation from 1 mm to 3 mm. Welding parameters and heat input of the welds are presented in table 2. Experimental welds were made with remelting with vacuum shielding gas. Welds were made on 5x100x100mm size plates. The heat input of electron beam welding was calculated using constant accelerating voltage 61 kV.

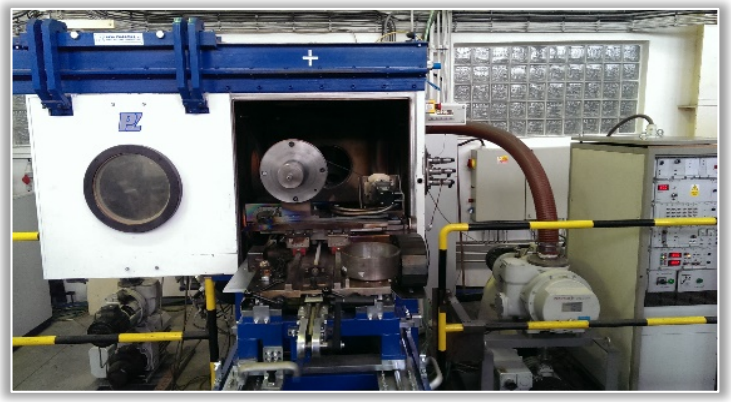

Figure 2. Universal electron beam welder PZ – EZ – ZH3

Table 2. Electron beam welding parameters

Number of sample	Average oscillation [mm]	Welding speed [mm.s^{-1}]	Welding current [mA]	Accelerating voltage [kV]	Heat input [kJ.mm^{-1}]
1.1	1	5	23	55	0,227
1.2	1	15	45	55	0,148
1.3	1	30	60	55	0,099
2.1	2	5	30	55	0,297
2.2	2	10	45	55	0,222
2.3	2	15	52	55	0,172
3.1	3	5	40	55	0,396
3.2	3	10	50	55	0,247
3.3	3	15	65	55	0,214

Oscillating the electron beam is an effective method to improve welding fusion and solidification, and increases the diameter of the keyhole. Beam oscillation prevents the molten envelopes from collapsing, and reduces the root spiking of the welds. Furthermore, beam oscillation increases the width of the fusion zone, and allows gas porosity to rise and escape from the weld pool mentioned Schultz [9].The amplitude of beam oscillation was from 1 mm to 3 mm, and the oscillating frequency was more than 200 Hz, which were optimum to weld by EBW. The functions of beam oscillation were circle illustrated in figure 3.

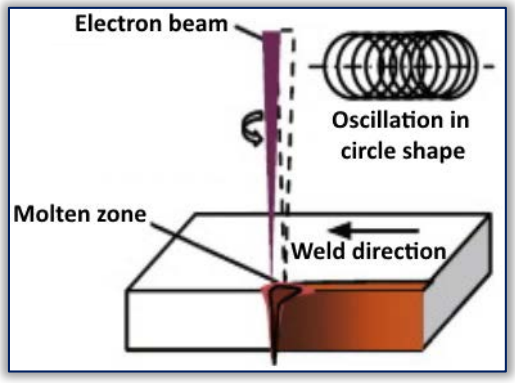

Figure 3. EBW with beam oscillation in circle shape [10]

— Structural investigation

The samples were cut from the weld plates and prepared for metallographic analyses by standard grinding and polishing and by etching with the Beraha reagent in proportion NH_4FHF 4,8 g – HCl 40 ml – H_2O 80 ml – $K_2S_2O_5$ 1 g. Macrostructural and microstructural analyses were carried out by optical and scanning electron microscopy (SEM). Distribution of elements in various areas of interface of samples was evaluated by high resolution scanning electron microscope JEOL 7600F with EDX analyser. Quantitative image analysis was performed on optical micrographs taken from the weld metal in order to calculate the ferrite and austenite volume fractions. The volume fractions of both ferrite and austenite

phases in EBW joints were determined using optical microscope loaded with commercial software program Image Analyzer. Microhardness measurements were also performed on the prepared samples, transversally to the weld axis and was performed using Vickers $HV_{0,1}$ measuring. For the detection of inside defects in the weld joints was used the ultrasonic testing Phased Array. The testing was carried out by the ultrasonic equipment Olympus OmniScan MX2 with the 5 and 10 MHz probes frequency.

3. RESULTS

— Macrostructural and microstructural analysis of welds

Cross-section macrostructure examination showed that the proper fusion of base metals was achieved while using EB welding and it is evident from figure 4 and 5. Welded joints made by changing the diameter of the beam oscillations (2-3 mm) are typical with barrel shape. The smaller average of the beam oscillation is used, the more it resembles the shape of the weld to the standard shape commonly observed during welding concentrated sources of energy.

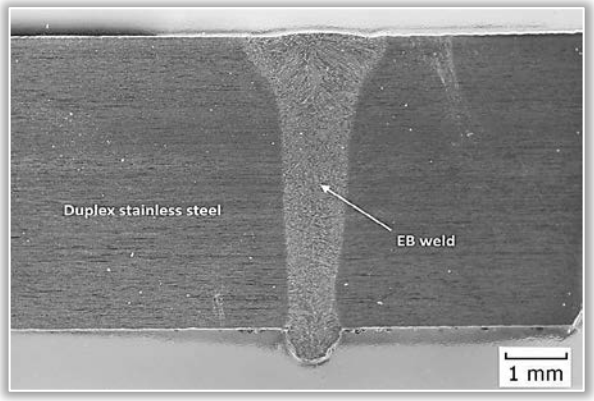

Figure 4. Macrostructure of cross-sectional view of the EBW joints with 30 mm.s^{-1} welding speed and average oscillation 1 mm

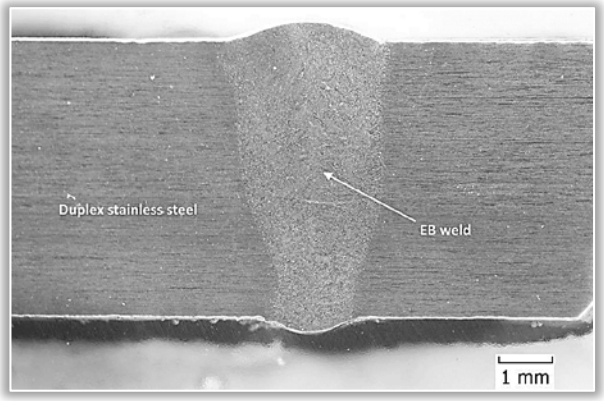

Figure 5. Macrostructure of cross-sectional view of the EBW joints with 10 mm.s^{-1} welding speed and average oscillation 3 mm

The details of microstructure investigation at various locations are presented in figures 6 and 7. Epitaxial and columnar grain growth is observed at the top region of the welds whereas the bottom end of the welds is showed like an equiaxed grains. The microstructure of the heat affected zone (HAZ) of DSS is similar to that of the base metal, with the presence of elongated α (ferrite) and γ (austenite) phases. In microstructure is not observed no atypical microstructural changes of HAZ and the proportions of the two phases are almost equal. Austenite excluded in the grain boundary is witnessed in the fusion zone which is acquainted to the faster cooling rates in the EBW process. The microstructure investigation revealed the presence of coarser ferrite grains with inter and intra-granular form of austenite which are dispersed in the ferritic matrix. EBW process employs faster cooling rate, the transformation product requiring higher degree of cooling, therefore intra-granular austenite is formed.

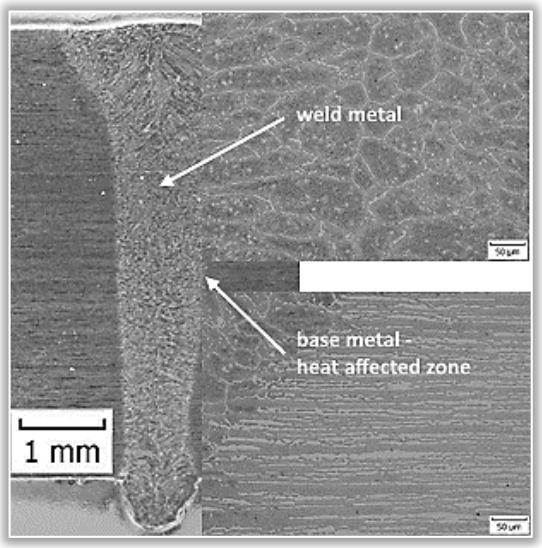

Figure 6. Microstructure of the EB welded duplex stainless steel plates (30 mm.s^{-1} welding speed and average oscillation 1 mm)

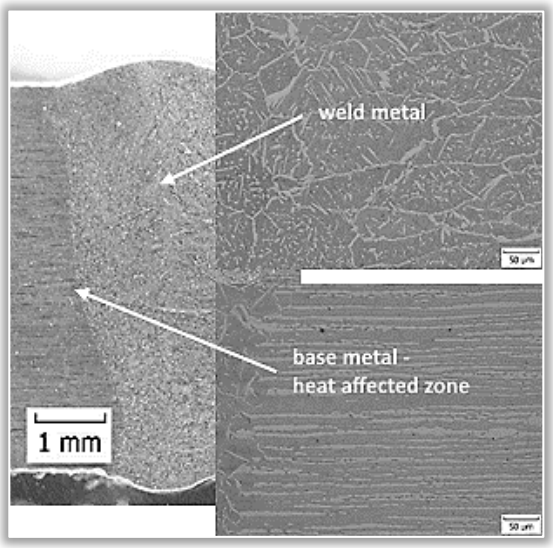

Figure 7. Microstructure of the EB welded duplex stainless steel plates (10 mm.s^{-1} welding speed and average oscillation 3 mm)

— **High resolution scanning electron microscope by EDX analyser**

Scanning electron microscope micrographs of the covering weld metal, root and the weld metal/HAZ interface, respectively, is shown in figure 8 a), b) and c). Figure 9 presents the chemical compositions of α phase and γ phase at the fusion zone of EB welds through the HAZ determined by SEM/EDAX analysis. The chemical composition of α phase (white regions) within the HAZ consists of 24,23 wt.% Cr, 3,79 wt.% Mo, 1,73 wt.% Mn, 8,41 wt.% Ni, 0,62 wt.% Si and 61,22 wt.% Fe, whilst the chemical composition of γ phase (grey regions) within the HAZ consists of 26,86 wt.% Cr, 6,08 wt.% Mo, 0,9 wt.% Mn, 5,28 wt.% Ni, 0,65 wt.% Si and 60,25 wt.% Fe. In the weld metal, the chemical composition of γ phase consists of 25,83 wt.% Cr, 6,18 wt.% Mo, 1,22 wt.% Mn, 7,47 wt.% Ni, 0 wt.% Si and 59,30 wt.% Fe whereas the α phase consists of 26,12 wt.% Cr, 6,15 wt.% Mo, 0,99 wt.% Mn, 6,83 wt.% Ni, 0,54 wt.% Si and 59,37 wt.% Fe. The EDX examinations indicate that partitioning of Cr, Ni and Mo between the ferrite and the austenite in the EB weld metal is not significant. It has been reported by some workers [11 -14] that there is no significant segregation of alloying elements in the final weld microstructure associated with the solid state phase transformation to austenite. This is due to rapid homogenization characteristic of ferritic solidification [12]. Ogawa and Koseki further indicated that the solid state transformation temperature range in the fusion zone of DSS occurs at about 1250-1150 °C. In this respect, the diffusion rate of Cr, Ni and Mo would be fairly decreased at that temperature range, thus resulting in insignificant partitioning of those elements between the ferrite and austenite phases. However, the transformation process of the weld is predominantly controlled by the diffusion of nitrogen, and this nitrogen is highly enriched in the austenite phase of the weld metal [12]. Therefore, it is believed that the austenite phase of the EB weld metal tends to contain more nitrogen than the ferrite phase. In table 3 is shown chemical compositions of different spectrums of EB weld.

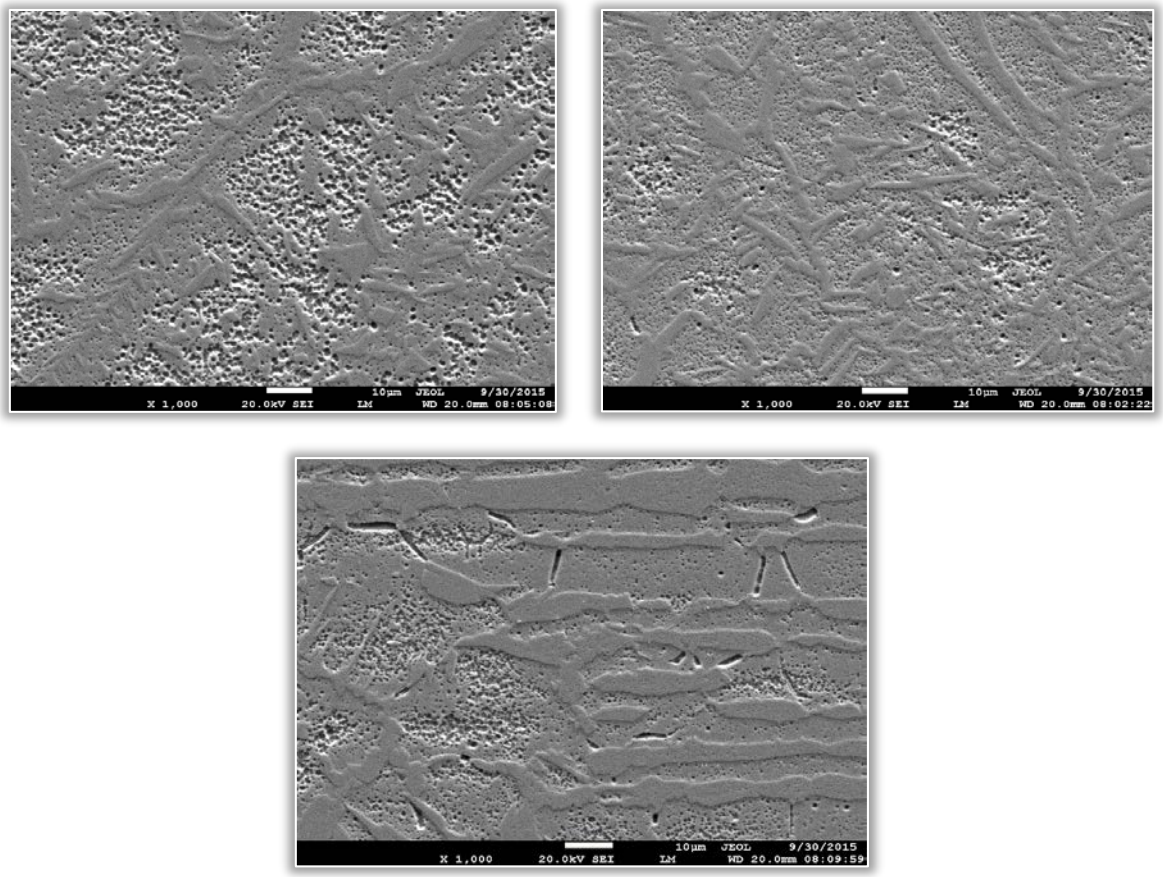

Figure 8. Scanning electron microscope of EB weld metal a) covering, b) root, c) weld metal/heat effected zone

Table 3. Chemical composition of different spectrums of EB weld

Spectrum	In stats.	Si	Cr	Mn	Fe	Ni	Mo	Total
Spectrum 1	Yes	0.54	26.12	0.99	59.37	6.83	6.15	100.00
Spectrum 2	Yes		25.92	1.13	60.23	6.49	6.24	100.00
Spectrum 3	Yes		25.83	1.22	59.30	7.47	6.18	100.00
Spectrum 4	Yes	0.65	26.86	0.90	60.25	5.28	6.08	100.00
Spectrum 5	Yes	0.62	24.23	1.73	61.22	8.41	3.79	100.00
Max.		0.65	26.86	1.73	61.22	8.41	6.24	
Min.		0.54	24.23	0.90	59.30	5.28	3.79	

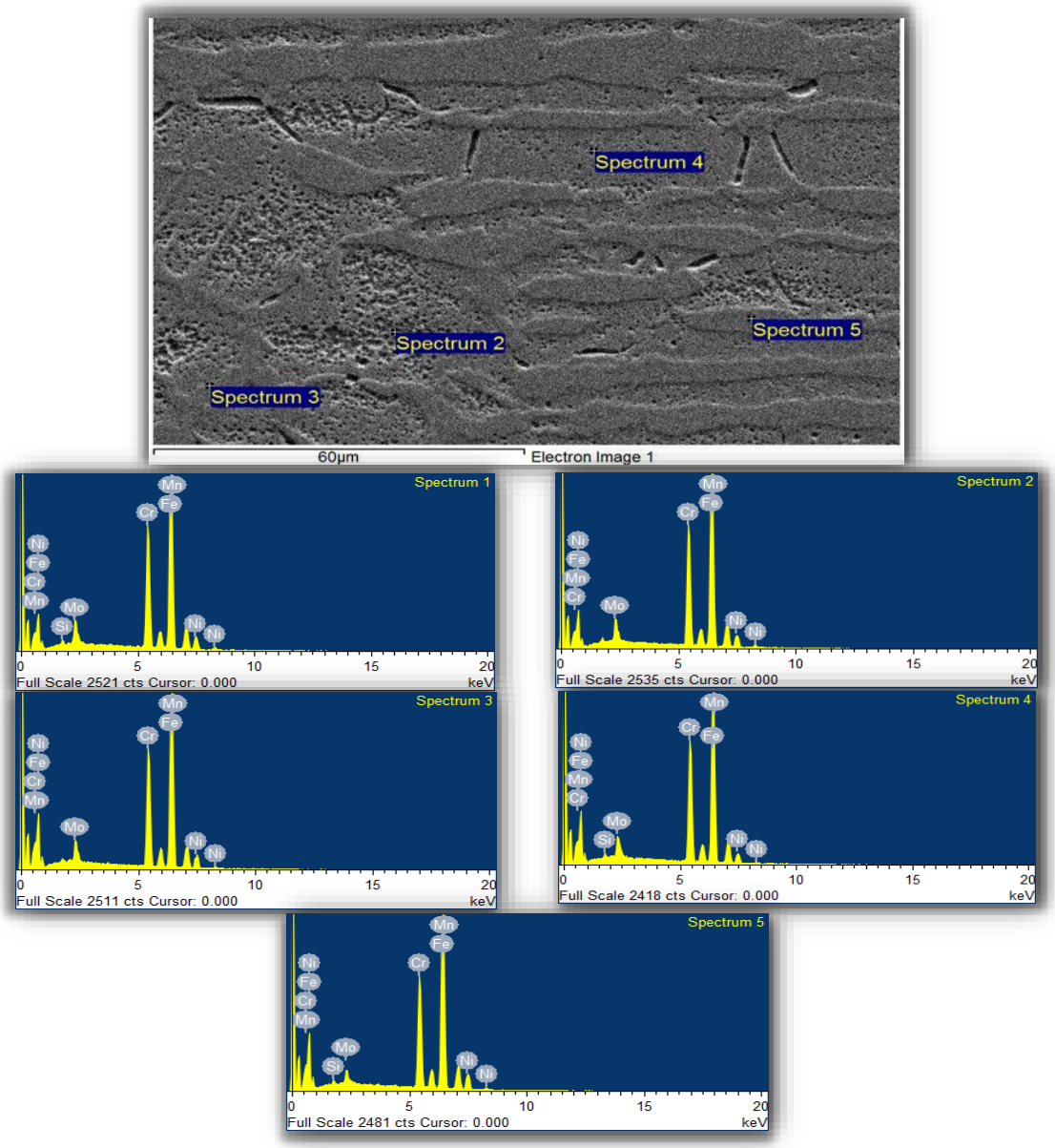

Figure 9. SEM/EDX point analysis representing the weld zones of duplex stainless obtained by EB welding

— **Ferrite content of duplex stainless steel welds**

Ferrite content of the welded joints is given in table 4. The results show that both weld metal composition, heat input and the cooling rate, together, decide the ferrite content. In comparison with EBW process using 1 mm average oscillation it can be argued that ferrite/austenite balance ratio in WM of EBW process using 3 mm average oscillation is closer to that of ferrite/austenite balance ratio in BM. This is related to higher heat input in the case of EBW process and faster cooling rate through the temperature transformation range. This means that the austenite volume fraction is remarkably influenced by heat input which is a function of welding process. These results agree qualitatively with optical metallography observations. The influence of beam oscillation on ferrite content shown in figure 10.

Table 4. Ferrite content of duplex stainless steel welds

Number of sample	Average oscillation [mm]	Welding speed [mm/s]	Heat input [k]/mm]	Ferrite content (%)
1.1	1	5	0,227	63,1
1.2	1	15	0,148	70,9
1.3	1	30	0,099	70,1
2.1	2	5	0,297	55,7
2.2	2	10	0,222	57,8
2.3	2	35	0,172	69,5
3.1	3	5	0,396	52,6
3.2	3	10	0,247	51,3
3.3	3	15	0,214	52,5

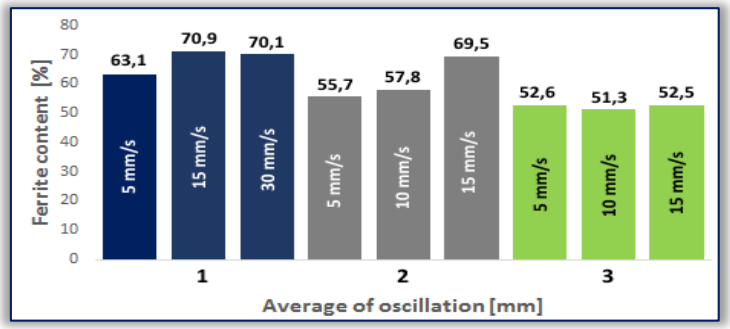

Figure 10. Histogram of ferrite content DSS welds made by EBW

— **Microhardness profile results**

Typical microhardness profiles of the welded joints with different heat input and average oscillation are shown on fig. 11. On the picture are documented average microhardness of samples 1. (1.1, 1.2, 1.3), 2. (2.1, 2.2, 2.3) and 3 (3.1, 3.2, 3.3). It is evident from these results that the smaller average oscillation and lower heat input to welds retained almost the same hardness as the base material about 280 HV. The greater average oscillation and input heat to welds had a higher hardness, values were obtained of over 303 HV near the centre of the welds. Figure 12 presents hardness measurement system of welded joints.

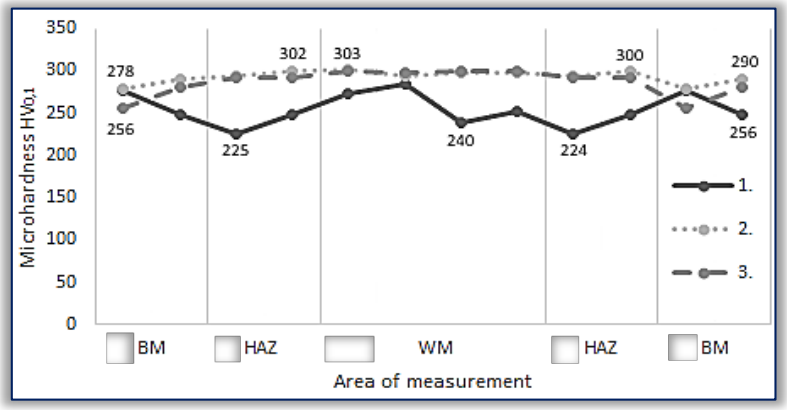

Figure 11. Profile of average microhardness across the welds

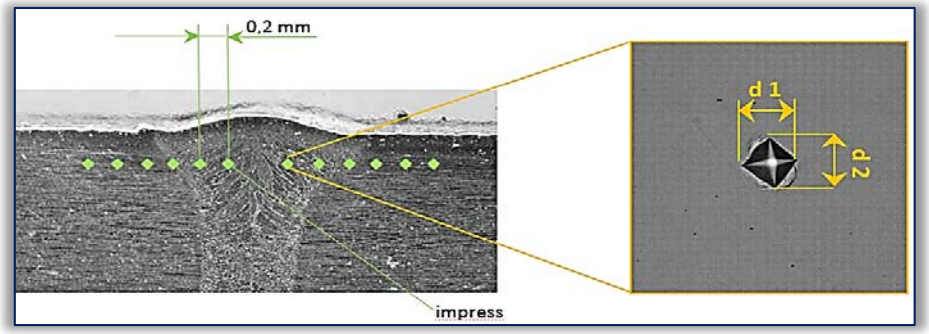

Figure 12. Microhardness measurement method

4. CONCLUSIONS

Electron beam welding (EBW) is well suited for thicker materials and enjoys the various advantages such as greater productivity, absence of secondary phases, a higher depth to width ratio, reduced residual stress and distortion, and the possibility of automation. On employing EBW for DSS, one of the serious problems addressed by Bonnefois [15] was that the ferrite–austenite ratio could be adversely affected as a result of the fast cooling rate and also the loss of nitrogen during welding. However the rapid cooling in EBW will be beneficial in suppressing the formation of inter-metallic precipitates.

— On the basis of analysis using light microscopy and scanning electron microscopy of DSS welds was found that the largest microstructural changes reflected in the weld metal during the laser welding process. Heat affected area was dull, on the grain boundaries of austenite and ferrite was observed precipitation of secondary phases. Similarly, the microstructure of the base material was not changed. It was made up of austenite and ferrite and the back were not observed excluded secondary phase.

— The microstructure of the EB weld metal is characterized by large ferrite grains with intra- and inter-

granular austenite. The austenite phase exhibits a needle-like structure and it is formed from ferrite in the solid state. HAZ consists of approximately equal proportions of the microstructure of the austenite and ferrite phases.

— EDX measurements indicate that there is no significant partitioning of Cr, Mo and Ni alloying elements in the austenite and ferrite phases of the weld metal.
— Ferrite content studies are showed that the ferrite–austenite balance ratio is maintained in the weld metal similar to base metal.
— The properties of DSS welded joints are dependent too on two factors namely mechanical properties and corrosion resistance. Mechanical properties was verified by microhardness measurement of DSS welded joints. Corrosion resistance and tensile test of DSS welding joints will be examined on the basis of future experiments.
— The welds of duplex stainless steel could be obtained from electron beam welding with well-established process parameters.
— The ultrasonic Phased Array testing of weld joints not confirmed the presence of defects, at the probe frequency of 10 MHz is seen considerable noise from the austenitic structure of the material.

Acknowledgements
We want to thank doc. ing. Mária Dománková, PhD. and ing. Ingrid Šutiaková for their useful comments and suggestions during this research.

References

[1] K. D. Ramkumara, D. Mishraa, M.K. Vignesha, B. G. Raja, N. Arivazhagana, S. V. Narena, S. S. Kumarb, Metallurgical and mechanical characterization of electron beam welded super-duplex stainless steel UNS 32750, Journal of Manufacturing Processes, vol. 16 (2014), no. 4, pp. 527–534.
[2] V. Muthupandi, P. B. Srinivasan, S.K. Seshadri, S. Sundaresan, Effect of weld metal chemistry and heat input on the structure and properties of duplex stainless steel welds, Materials Science and Engineering A, vol. 358 (2003), no. 1-2, pp. 9-16
[3] H.D. Solomon, T.M. Devine Jr., Duplex stainless steels: A tale of two phases, Proceedings of the Conference on Duplex Stainless Steels, ASM, St. Louis, 1982, pp. 693– 756.
[4] Bonnefois, B., Charles, J., Dupoiron, F. and Soulignac, P., How to predict welding properties of duplex stainless steels, Proceedings of the conference on Duplex Stainless Steels '91, Beaune (France), vol. 1 (1991), pp. 347-361.
[5] J.C. Lippold, W. Lin, S. Brandi, I. Varol, W.A. Baeslack, Heat affected zone microstructure and properties in commercial duplex stainless steels, Proceedings of the Fourth International Conference on Duplex Stainless Steels, Glasgow, Scotland, vol. 2, (1994), Paper 116.
[6] J. Charles, The Duplex Stainless Steels: Material to meet your needs, Proceedings of the Conference on Duplex Stainless Steels '91, Beaune (France), vol. 1 (1991), pp. 3 – 48.
[7] Schwarz L, Vrtochová T, Ulrich K. Laser beam welding of superduplex stain-less steel with post weld heat treatment, https://www.mtf.stuba.sk/buxus/docs/internetovy_casopis/2010/3/schwarz_vrtochova_ulrich.pdf
[8] ASM handbook on mechanical testing and evaluation, ASM International, vol. 8. (2000).
[9] H. Schultz., Electron beam welding (4rd ed.), Elsevier, Cambridge (2003).
[10] F. Pengfeia, M. Zhiyongb, Z. Congjinb, W. Yajunc, W. Chunming, Microstructures and fatigue properties of electron beam welds with beam oscillation for heavy section TC4-DT alloy, Chinese Journal of Aeronautics, vol. 27 (4) (2014), pp. 1015-1021.
[11] T. Ogawa and T. Koseki, Composition Profiles on Metallurgy and Corrosion Behavior of Duplex Stainless Steel Weld Metals, Welding Journal, vol. 68 (5) (1989), pp.181-191.
[12] N. Suutala, T. Takalo and T. Moisio, Single phase ferritic solidification mode in austenitic-ferritic stainless steel welds, Metallurgical Transactions A, vol. 10 (1979), pp. 1183–1190.
[13] N. Suutala, T. Takalo, and T. Moisio, The relationship between solidification and microstructure in austenitic and austenitic-ferritic stainless steel welds, Metallurgical Transactions A, vol. 10 (1979), pp.512-514.
[14] W. T. DeLong, Ferrite in austenitic stainless steel weld metal, Welding Journal, vol. 53 (7) (1974), pp. 273-286.
[15] Bonnefois B, Soulignac A, Charles J., Some Aspects of Nitrogen Introduction in the Duplex Weld Pool, Proceedings of the conference on Duplex Stainless Steels '91, Beaune (France), vol. 1. (1991), pp. 469–478

ISSN 1584 – 2665 (printed version); ISSN 2601 – 2332 (online); ISSN-L 1584 – 2665
copyright © University POLITEHNICA Timisoara, Faculty of Engineering Hunedoara,
5, Revolutiei, 331128, Hunedoara, ROMANIA
http://annals.fih.upt.ro